ELSEVIER

Polymer 43 (2002) 6695–6700

polymer

www.elsevier.com/locate/polymer

Calculation of mesophase percentage of polymer fibers from 2D wide-angle X-ray scattering patterns

Jing Wu[a,*], Jerold M. Schultz[b]

[a]*Department of Chemical Engineering, New Jersey Institute of Technology, Newark, NJ 07102, USA*
[b]*Department of Chemical Engineering, University of Delaware, Newark, DE 19716, USA*

Received 10 May 2002; received in revised form 10 September 2002; accepted 12 September 2002

Abstract

A computational method is developed to evaluate the relative amount of mesophase of polymer fibers from their two-dimensional (2D) wide-angle X-ray scattering (WAXS) patterns. This is achieved by first evaluating the percentage of oriented phases (POPs) from a 2D WAXS pattern. If there exists a crystalline phase, crystallinity is subtracted from the POPs to obtain the mesophase percentage. If no crystalline phase is observed from a WAXS pattern, the POPs is the mesophase percentage. To increase the computation accuracy, a center search algorithm is developed and a Fourier filter is adapted to perform data smoothing. The Bresenham midpoint circle algorithm is applied to accelerate the computation.

This method is applied to compute the mesophase percentages of poly(trimethylene terephthalate) (PTT) fibers of take-up speeds ranging from 970 to 4185 m/min. Our results indicate that the mesophase percentage increases with take-up speeds up to 2550 m/min. With further increase in take-up speeds, the mesophase percentage begins to drop. This is because the mesophase is precursory to the crystalline phase and is depleted by the formation of the crystalline phase during spin-line stress-induced crystallization in the take-up speed range of 3050 to 4185 m/min. This finding is consistent with results on PET fibers.

Keywords: Mesophase percentage; Center search for WAXS patterns; Bresenham midpoint circle algorithm

1. Introduction

During the last two decades, it became understood that transitions of a semicrystalline polymer from its molten state to crystalline state can proceed through intermediate states. In the case of highly oriented material, the intermediate state is termed an "oriented mesophase" [1]. This terminology derives from studies of poly(ethylene terephthalate) (PET) fibers.

The first work suggesting the existence of an intermediate phase came from NMR studies in the 1970s by Eichhoff and Zachmann [2]. Typically, the broad component of an NMR scan is ascribed to immobile chain segments of the crystalline phase, while the narrow component is attributed to mobile segments of an amorphous phase. Eichhoff and Zachmann showed that swelling of PET transferred a portion of the broad NMR signal to the narrow component, while causing no change in the intensity of the corresponding crystalline wide-angle X-ray scattering (WAXS) [2]. Therefore, the transformed part of the broad NMR portion must represent an immobile noncrystalline phase. Later, using NMR, WAXS and small-angle X-ray scattering measurements on PET fibers, Biangardi and Zachmann [3–6] showed that the immobile noncrystalline phase consists of straight and highly oriented chain segments. It was separately noted by Lindner [7] that the amorphous halo in oriented PET fibers consists of a random component and a highly oriented component, suggesting the existence of oriented noncrystalline chains.

On the basis of these results, it was suggested by Gupta and Kumar [1] that an intermediate phase, termed the "oriented mesophase", exists. This intermediate state between crystalline and amorphous states can be used to refer to a wide spectrum of intermediate structures, ranging from stiff chains with no long-range registry [3–6] to poorly formed crystals [1,7]. There is not a clear boundary to delineate these regions. This situation is sketched in Fig. 1.

Shimizu et al. [8] related the formation of the mesophase in PET fibers to processing history. Fu et al. [9–12] noted a

* Corresponding author.
E-mail addresses: jingwu@adm.njit.edu (J. Wu), schultz@che.udel.edu (J.M. Schultz).

0032-3861/02/$ - see front matter
PII: S0032-3861(02)00672-9

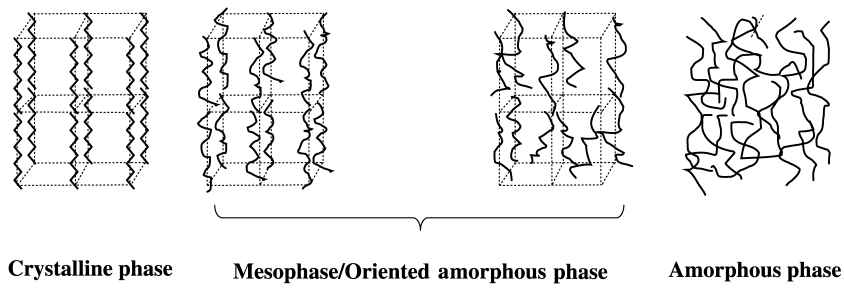

Fig. 1. An illustration of a wide range of possible structures of mesophase.

consistent discrepancy between measured and calculated WAXS profiles from PET fibers. This discrepancy was attributed to the scattering from the mesophase. Hsiao et al. observed a similar behavior during a synchrotron on-line study of the melt spinning of nylon 66 [13]. More recently, the mesophase development in polypropylene fibers was studied by Ran et al. [14–16].

Although the existence and the importance of the mesophase have been widely acknowledged, there are few methods developed to represent its characteristics. Using azimuthal scans on a 2D WAXS pattern, Murthy and coworkers suggested a way of computing the mesophase orientation [17,18], and evaluating the mesophase percentage [19]. Their approach uses peak height at the amorphous halo as the basis of the computation. Strictly speaking, the rigorous approach to compute mesophase percentage should use peak area instead of merely the intensity maximum at the scattering angle corresponding to the position of the amorphous halo. In other words, the scattering contribution of the mesophase at each scattering angle should be accounted for. Probably, the difficulty in separation of mesophase scattering from that of crystalline or amorous phase prohibited Murthy et al. from using this approach. This difficulty lies in the fact that the mesophase possesses a nonclassical degree of order. The frequency characteristic of its scattering curve may be similar to that of poorly formed crystals or of the amorphous phase, depending on processing details. Consequently, it is inherently difficult to separate the scattering of the mesophase from that of crystalline or amorphous phases using a standard Fourier filter alone.

Fu et al. obtained scattering solely from the mesophase by optimization of crystal structure and subsequent removal of crystalline scattering [9–12]. The undesired aspect of this approach is that crystal structures are not optimized against scattering from the crystalline phase alone; instead they are optimized against scattering from crystalline and mesophase phases. Therefore, this approach requires initial guesses of unit cell dimensions to be very close to the true values. This limits its application to situations in which initial guesses are not accurate. Other efforts to compute mesophase percentage include Murthy and Zero's [20] two-dimensional (2D) fitting of the oriented amorphous halo, which is also implemented in the Fit-2D package from ESRF.

In this research, an algorithm is developed to compute the mesophase percentage from 2D WAXS patterns. This method is not based on a direct separation of scattering contributions from the mesophase. Instead, the orientation characteristic of the scattering from the mesophase is exploited as the basis of the method. Comparing with Murthy's method, our approach accounts for the scattering of mesophase at all scattering angles and is therefore more rigorous. It is applicable whether a crystalline phase exists. Therefore, it is capable of computing the mesophase percentage in oriented noncrystalline or crystalline polymer systems. It is worthwhile to note that some publications [21,22] dedicated the term mesophase to refer to a specific low energy form of noncrystalline phase. Other researchers, on the other hand, used mesophase to refer to a broad range of oriented noncrystalline phases, including the low-energy form [1,7,15]. Since our approach is applicable to all these phases, the latter convention is adopted.

As an example, WAXS patterns of poly(trimethylene terephthalate) (PTT) fibers spun using take-up speeds ranging from 970 to 4185 m/min have been subjected to analysis using this algorithm.

PTT is a recent phenomenon in polymer industry. It was commercialized by Shell via an affordable monomer process in 1995, and is now entering fiber and thermoplastics application fields. Because of its excellent resiliency, PTT is an ideal material for textile and carpet applications. The processing window of PTT fibers is, however, quite narrow. Particularly, the processing window for drawing of PTT as-spun fibers is very narrow and greatly dependent upon take-up speeds. It is suspected that the mesophase fraction in PTT fibers affects the drawing window. This is the motivation for development of this algorithm to quantify the mesophase fraction of PTT fibers.

2. Principles for the determination of mesophase percentage

This method is based on the orientation feature of 2D WAXS patterns from polymers fibers. In such patterns, one knows that the crystalline scattering intensities for specific (hkl) crystal planes appear at specific scattering angles and azimuthal angles. The scattering angle is determined by Bragg's law and the azimuthal angle is determined by the orientation distribution of the crystallites. On the other hand,

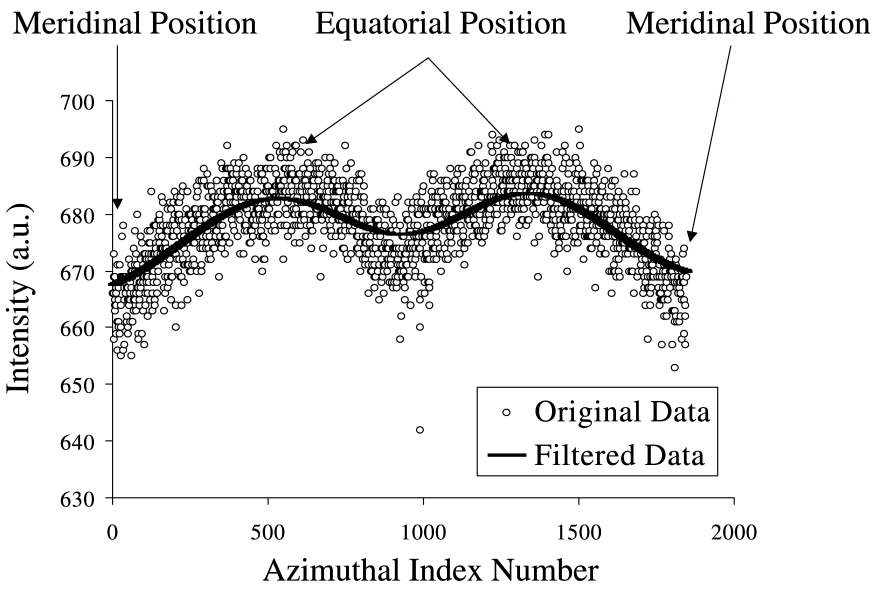

Fig. 2. Azimuthal intensity profile at a radial position showing the existence of the mesophase.

amorphous scattering exhibits itself as an amorphous halo, a broad, azimuthally uniform hump around a certain scattering angle. If there exists a mesophase, its scattering characteristics will be similar to that of the amorphous phase, except that stronger intensity will appear on the equator than on the meridian. Such a situation is shown in Fig. 2, in which an azimuthal scan at $2\theta = 12.2°$ is plotted. There is no crystalline scattering at this scattering angle.

If an azimuthal scan is performed on a background-corrected pattern at a specific scattering angle, the baseline is due to the scattering from amorphous phase, while peaks come from the scattering from oriented phases such as crystalline and mesophase. When this operation is performed for all scattering angles, the percentage of oriented phases (POPs) can be calculated according to the following equation

$$\mathrm{POP} = \frac{\sum_{\text{Scattering angles}} \begin{array}{c}\text{Area above the baseline of an}\\ \text{azimuthal scan at a scattering angle}\end{array}}{\sum_{\text{Scattering angles}} \begin{array}{c}\text{Total area of an azimuthal scan}\\ \text{at a scattering angle}\end{array}} \quad (1)$$

This equation is based on the principle for determining crystallinity from WAXS patterns [23,24], and is an extension of the method proposed by Murthy [19].

After determining the POP, the mesophase percentage is determined as follows. If there exists crystalline phase in the polymer fiber, the crystallinity is subtracted from the POP and the percentage of the mesophase is obtained. If no crystalline phase is observed from WAXS, the POP is the mesophase fraction. The crystallinity is determined via peak deconvolution of the one-dimensional (1D) intensity profile obtained by azimuthal integration of 2D WAXS patterns obtained over a range of azimuthal angles. A detailed procedure for crystallinity calculation can be found elsewhere [23,24]. As a result of azimuthal integration, the intensity contribution from poorly formed crystals and intracrystalline defects is added to the amorphous portion. Therefore, crystallinity determined in this way is the lower limit of the fraction of crystalline phase. The difference between POP and crystallinity determined in this way is the fraction of the noncrystalline oriented phase (i.e., the mesophase).

3. Computational aspects

In order to accurately and efficiently evaluate the mesophase fraction, the following routines are developed or adapted.

(a) Center search and Fourier smoothing of original data.
(b) Bresenham midpoint circle algorithm [25,26].

3.1. Center search

Imaging plates are frequently used to collect X-ray scattering data. Since an imaging plate needs to be removed from its collecting position for digitization and restoration after each exposure, the center of a pattern, i.e., the primary beam position on an imaging plate, is not known in a priori and has to be determined separately for each scan. If crystalline diffraction spots are observed, the center can be readily determined from the symmetrical scattering spots. For patterns from air background or noncrystalline samples, however, it is extremely hard to determine the center of such patterns. This situation is even worse if a central hole is cut on an imaging plate to allow the passage of small-angle scattering signals. The existing methods for center determination, i.e. 2D fit of low-angle intensity to extrapolate

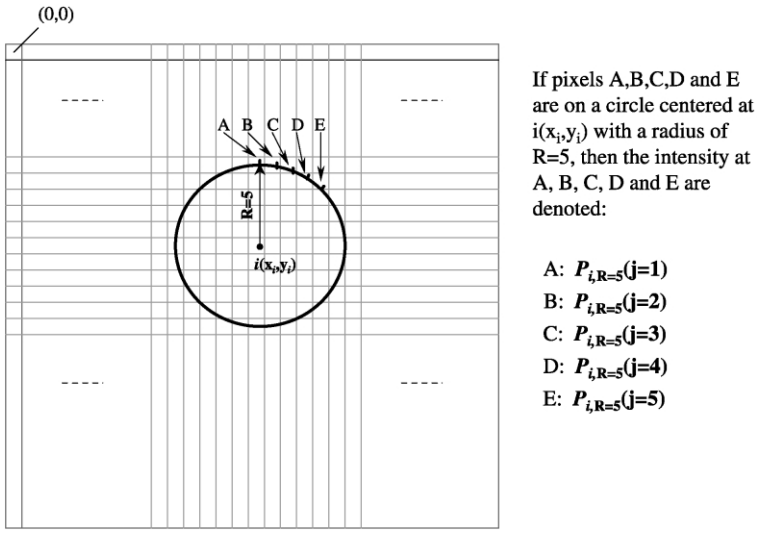

Fig. 3. An illustration of $P_{i,R}(j)$ and its parameters i, j, R on an imaging plate.

primary beam position and the use of Hugh transform [27], usually cannot allocate an accurate center.

Our solution to this problem is a center search algorithm, which is based on the observation that the air background scattering should be isotropic around the center. The key of this search algorithm is to define an isotropic parameter for a point on an imaging plate. Then a region that contains the true center is defined and the isotropic parameter for each point in the region is evaluated. The point with the smallest isotropic parameter is the true center.

To define the isotropic parameter for a specific point i, the following notations will be used.

(x_i, y_i) the coordinate of the point, i, on the imaging plate using pixel units, with the upper left corner of the imaging plate as $(0, 0)$

$P_{i,R}(j)$ the azimuthal intensity profile about the point i at a certain radius R, with j being the index of the intensity profile array, starting from the meridian. Fig. 3 shows $P_{i,R}(j)$ and its parameters i, j, R on an imaging plate.

Note that the coordinates of the points on this azimuthal profile, (x, y), must satisfy

$$(x - x_i)^2 + (y - y_i)^2 = R^2 \tag{2}$$

The isotropic parameter for point i at radius R, $\mathrm{Iso}(i, R)$ is then defined as

$$\mathrm{Iso}(i, R) = \sum_j [P_{i,R}(j) - P_{i,R}(j + 1)]^2 \tag{3}$$

In Eq. (3), the limit of j is equal to the array length of the azimuthal intensity profile around point i at radius R. It is on the order of $R/\sqrt{2}$. In the implementation, the array length is dynamically counted.

The isotropic parameter for point i, $\mathrm{Iso}(i)$, is given by,

$$\mathrm{Iso}(i) = \sum_R \mathrm{Iso}(i, R) \tag{4}$$

In order to reduce the computation expense, selected R values may be used in Eqs. (3) and (4).

The above algorithm is applicable to air background patterns, patterns from amorphous polymers, and patterns from noncrystalline polymers with the existence of a mesophase. In all cases, the isotropic parameter about an erroneous center possesses a much larger value than that about the true center. One should note that the ideal isotropic parameter about the true center in the first two cases should be zero, while that in the last case is nonzero because azimuthal intensity distribution around the true center is not uniform due to chain orientation.

3.2. Fourier smoothing of original data

After the determination of the center of a pattern, the original data is converted into azimuthal scans at consecutive scattering angles, and subsequently smoothed by a Fourier filter to reduce data noise. The frequency range of the Fourier filter is adjusted such that most of the noise can be removed without losing crystalline scattering peaks. Our implementation is based on a routine from Numerical Recipe in C [28]. The original data and filtered data are shown in Fig. 2.

3.3. Bresenham midpoint circle algorithm

It is noted that the azimuthal profiling is constantly used in the center search and Fourier smoothing. In order to perform azimuthal profiling, it is necessary to compute the y coordinate, given the x coordinate, using Eq. (2), or vice versa. When Eq. (2) is solved for y given x, y must be rounded to an integer, because the

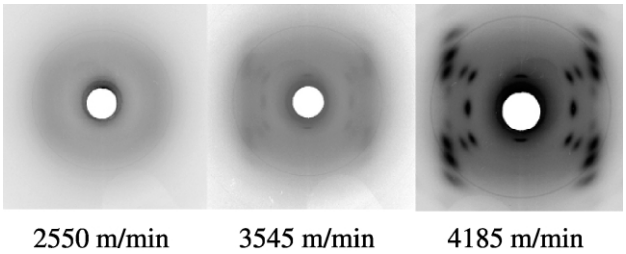

Fig. 4. Three representative WAXS patterns from PTT fibers prepared at different take-up speeds.

coordinates are integers. This process, along with the floating point calculation when solving Eq. (2), is computationally expensive if Eq. (2) is to be solved many times, which is the case during center search or Fourier smoothing. To see this, for center search in a 50 pixel × 50 pixel region and to compute the isotropic center for 10 radii, Eq. (2) is to be solved 25,000 times.

While the number of times needed to solve Eq. (2) cannot be changed, the overhead of solving Eq. (2) can be significantly reduced by using the Bresenham midpoint circle algorithm [25,26]. Solving Eq. (2) is equivalent to determining whether a point (x, y) is on the circumference of a circle. The Bresenham midpoint circle algorithm achieves this goal with only integer arithmetic involved. It is incremental in nature; that is, by using the result at (x_p, y_p), determining if the next point is on the circumference. Since this algorithm is not widely used in the X-ray community, it is worthwhile to note that it helps to save significant computational expenses.

4. Implementation: the mesophase fraction of PTT fibers

To demonstrate this method, the relative amount of mesophase of a series of PTT as-spun fibers is evaluated. The take-up speeds of these fibers range from 970 to 4185 m/min. A detailed description of these fibers and the WAXS experiment can be found elsewhere [29]. Three

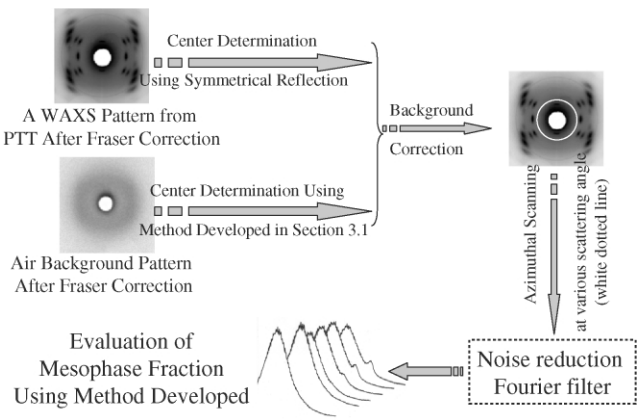

Fig. 5. Computation procedure for evaluation of mesophase fraction.

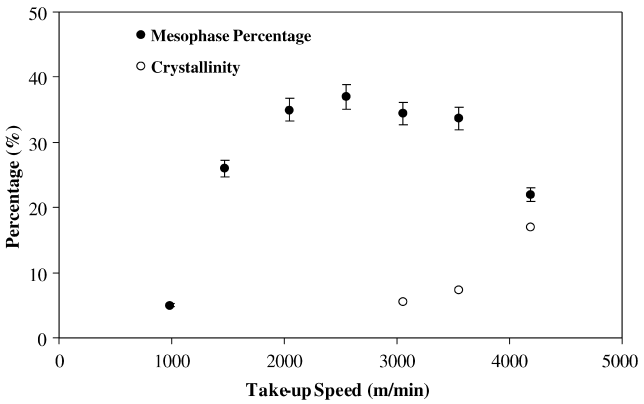

Fig. 6. Dependence of percentage of mesophase and corresponding crystallinity on take-up speed of PTT fibers.

representative WAXS patterns are shown in Fig. 4. Since the WAXS patterns were registered on a flat-plate detector, the curvature of the Ewald sphere was corrected after Fraser [30] using the software, X-ray Diffraction Processing Package (XDPP), developed by Hsiao.

The centers of these patterns and the corresponding air background patterns are determined using either symmetrical reflections or the method described in Section 3.1. Then air backgrounds are scaled and subtracted such that its low-angle portion matches that of a sample scattering pattern. Azimuthal scans at each scattering angle are performed on the background-corrected patterns and the noises of these scans are reduced by passing these scans through the Fourier filter described in Section 3.3. The 2θ range is from 3.5 to 33.5°. The mesophase fraction is then evaluated using the noise-reduced azimuthal scans according to the procedure developed in Section 2. The computational procedure is shown in Fig. 5.

The computed mesophase fraction and the corresponding crystallinity are plotted in Fig. 6. The crystallinity was determined according to a procedure previously described [29].

From Fig. 6, one observes that the mesophase fraction increases with take-up speeds up to 2550 m/min. With further increase in take-up speed, the mesophase fraction begins to drop. This is because the mesophase is precursory to the crystalline phase and is depleted by the formation of the crystalline phase during spin-line stress-induced crystallization in the take-up speed range of 3050 to 4185 m/min. Similar behavior was also observed for PET [8].

The crucial part of the computational procedure shown in Fig. 5 is to adjust the Fourier filter for data smoothing. The frequency range of the Fourier filter is adjusted such that most of the noise can be removed without losing crystalline scattering peaks. The errors in the mesophase percentage can be decomposed into random error and systematic error. The random error is introduced due to the error in scattering pattern center determination and background correction. Using multiple computational experiments, the random

error is confined below 5%. There are two major sources of systematic errors. One is introduced via the missing meridianal reflections of WAXS patterns of fibers. For PTT system, this error is less than 5%, as the contribution of the (002) reflection, the only meridianal reflection of PTT, is small [31]. Another systematic error is introduced during data smoothing. When the frequency range of the Fourier filter is adjusted, the mesophase percentage curve shifts up and down as a whole. The frequency range of the Fourier filter is carefully adjusted through multiple computation and visual inspection such that the random noise can be eliminated without losing fine signals from crystalline scattering. In our computation, the parameter which controls the frequency range of the filter is set to 1/32 of the data array size. This parameter is used for all patterns.

5. Conclusion

A full-pattern computational algorithm is developed to evaluate mesophase fraction in oriented polymer systems from 2D WAXS patterns. This algorithm is demonstrated using 2D WAXS patterns from a series of PTT as-spun fibers.

Acknowledgements

We acknowledge the financial support by NSF GOALI Grant DMR-9629825. We are indebted to Prof. B. Hsiao for providing access to XDPP software at SUNY-SB. Additionally, JW gratefully acknowledges the financial support in part by SBR Grant Program of New Jersey Institute of Technology, Grant no. 421880.

References

[1] Gupta VB, Kumar S. Polymer 1978;19(8):953–5.
[2] Eichhoff U, Zachmann HG. Makromol Chem 1971;147:41–51.
[3] Biangardi HJ, Zachmann HG. Makromol Chem 1976;177:1173–84.
[4] Biangardi HJ, Zachmann HG. J Polym Sci, Polym Symp 1977;58: 169–83.
[5] Biangardi HJ, Zachmann HG. Prog Colloid Polym Sci 1977;62: 71–87.
[6] Biangardi HJ. Prog Colloid Polym Sci 1979;66:99–108.
[7] Lindner WL. Polymer 1973;14(1):9–15.
[8] Shimizu J, Kikutani T, Takaku A, Proceedings of the International Symposium on Fiber Science, Hakone, Japan. Barking, Essex: Elsevier Applied Science; 1985. August 20–24.
[9] Fu Y, Annis B, Boller A, Jin Y, Wunderlich B. J Polym Sci, Part B, Polym Phys 1994;32(13):2289–306.
[10] Fu Y, Busing WR, Jin Y, Affholter KA, Wunderlich B. Macromol Chem Phys 1994;195:803–22.
[11] Fu Y, Busing WR, Jin Y, Affholter KA, Wunderlich B. Macromolecules 1993;26:2187–93.
[12] Chen W, Fu Y, Wunderlich B, Cheng J. J Polym Sci, Part B, Polym Phys 1994;32(16):2661–6.
[13] Hsiao BS, Kennedy AD, Leach RA, Barton RJ, Harlow R, Ross R, Seifert S, Zachmann HG. Polym Prepr (Am Chem Soc, Div Polym Chem) 1995;36(1):340–1.
[14] Ran S, Zong X, Fang D, Hsiao BS, Chu B, Ross R. J Appl Crystallogr 2000;33(4):1031–6.
[15] Ran S, Zong X, Fang D, Hsiao BS, Chu B, Cunniff PM, Phillips RA. J Mater Sci 2001;36(13):3071–7.
[16] Ran S, Zong X, Fang D, Hsiao BS, Chu B, Phillips RA. Macromolecules 2001;34(8):2569–78.
[17] Murthy NS, Correale ST, Moore RAF. J Appl Polym Sci, Appl Polym Symp 1991;47:185–97.
[18] Murthy NS, Minor H, Bednarczyk C, Krimm S. Macromolecules 1993;26(7):1712–21.
[19] Murthy NS, Bray RG, Correale ST, Moore RAF. Polymer 1995; 36(20):3863–73.
[20] Murthy NS, Zero K. Polym Commun 1997;38:2277.
[21] Jakeways R, Klein JL, Ward IM. Polymer 1996;37(16):3761–2.
[22] Auriemma F, Corradini P, De Rosa C, Guerra G, Petraccone V, Bianchi R, Di Dino G. Macromolecules 1992;25(9):2490–7.
[23] BaltaCalleja FJ, Vonk CG. X-ray scattering of synthetic polymers. Amsterdam: Elsevier; 1989.
[24] Wu J, Schultz J, Yeh F, Hsiao B, Chu B. Macromolecules 2000;33: 1765–77.
[25] Bresenham JE. Commun ACM 1977;20(2):100–6.
[26] Foley JD, Dam A, Feiner SK, Hughes JF, Phillips RL. Introduction to computer graphics. New York: Addison-Wesley; 1994.
[27] Dammer C, Leleux P, Villers D, Dosiere M. Nucl Instrum Meth Phys Res, Sec B: Beam Interact Mater Atoms 1997;132(1):214–20.
[28] Press WH, Teukolsky SA, Vetterling WT, Flannery BP. Numerical recipes in C: the art of scientific computing. New York: Cambridge University Press; 1988.
[29] Wu J, Schultz J, Samon J, Pangelinan A, Hoe C. Polymer 2001;42: 7161–70.
[30] Fraser RDB, MacRae TP, Miller A, Rowlands RJ. J Appl Crystallogr 1976;9:81–94.
[31] Desborough IJ, Hall IH, Neisser JZ. Polymer 1979;20(5):545–52.